

Percolation in binary mixtures with strong attraction between unlike particles

This article has been downloaded from IOPscience. Please scroll down to see the full text article.

1991 J. Phys.: Condens. Matter 3 5603

(<http://iopscience.iop.org/0953-8984/3/29/013>)

View [the table of contents for this issue](#), or go to the [journal homepage](#) for more

Download details:

IP Address: 171.66.16.147

The article was downloaded on 11/05/2010 at 12:23

Please note that [terms and conditions apply](#).

Percolation in binary mixtures with strong attraction between unlike particles

Jun Wang†§, I L McLaughlin† and M Silbert‡

† Department of Physics, La Trobe University, Bundoora, Victoria, Australia 3083

‡ School of Physics, University of East Anglia, Norwich NR4 7TJ, UK

Received 18 January 1991, in final form 15 April 1991

Abstract. The percolation and clustering in binary mixtures with strong attraction between unlike particles is investigated. More specifically, we consider a binary mixture in which the interaction between unlike particles is described by Baxter's sticky hard sphere (SHS) potential, while the interaction amongst the same species is the hard sphere repulsion. The Ornstein–Zernike (OZ) equation for the pair connectedness is solved under the Percus–Yevick (PY) approximation. The percolation line always approaches zero as the density vanishes and also percolation only occurs above some lower limit of density. The percolation line is compared with the phase transition line and it is found that the existence of the phase transition line restricts the range of concentration for which percolation occurs. Moreover, the influences of density, stickiness, concentration and particle size on the pair connectedness, percolation line, mean cluster size and the coordination number are examined.

1. Introduction

The study of clustering and percolation behaviour in disperse particles is related to a wide range of phenomena; of these we are particularly concerned with the behaviour of dispersion of strongly interacting macroparticles, e.g. colloids. Although there are problems with the precise definition on what constitutes a physical cluster [1], the one introduced by Hill [2] (see below) has been widely used in the literature. Coniglio *et al* [3,4] used Hill's concept of a physical cluster to derive a general expression for the average number of physical clusters in a system in order to study the equilibrium distribution of these clusters and develop a theory of the pair connectedness for one component systems.

In analogy with the pair correlation function in liquid theory, the central quantity in Coniglio's approach is the pair connectedness function $p(r)$, which is proportional to the probability that two particles belong to the same cluster with a separation of r . Coniglio *et al* [4] obtained an Ornstein–Zernike (OZ) integral equation and Percus–Yevick (PY) closure for the pair connectedness functions as well as the expression of the mean cluster size for continuous systems, which is the key to finding the percolation threshold, i.e. the density at which an infinite cluster forms.

Following the work by Coniglio *et al*, percolative behaviour has been investigated for different systems and the OZ equation has been solved both analytically and

§ On leave from Physics Department, Henan Normal University, Xinxiang, Henan, People's Republic of China.

numerically, and compared with computer simulations. Analytic solutions of the connectedness from the OZ equation in the PY approximation for permeable spheres and sticky hard sphere (SHS) systems have been obtained by Chiew and Glandt [5]. Demisone *et al* [6] solved the OZ equation in the same approximation analytically for extended spheres. Xu and Stell [7] determined the pair connectedness function and the percolation threshold for a system interacting via a pair potential with a hard core and Yukawa tail in the mean spherical approximation. Numerical methods have been used by Netemeyer and Glandt [8] to examine the percolation of square well fluids. Monte Carlo simulations of percolation have been carried out for several systems; e.g. the SHS by Seaton and Glandt [9, 10], and the square well by Chiew and Wang [11].

More recently there have been extensions of the above studies to the case of binary mixtures. Chiew and Stell [12] have extended the formalism of Coniglio *et al* to mixtures. The model potentials used in their study are randomly centered and permeable spheres. The influences of density on the pair connectedness functions and concentration on the percolation thresholds were examined. Wu and Chiew [13] studied the percolation in binary mixtures of randomly centered spheres when particle clustering is selective, that is, only particles of different species are allowed to be physically bound. They found that the percolation threshold depends on concentration, while for the non-selective case it does not.

More recently, Chiew and Glandt [14] discussed the percolation in binary mixtures of SHS, where sticky attractions only occur among like species with hard sphere repulsion between unlike particles. They determined the analytical expressions for the pair connectedness and the mean cluster size and then examined the influences of different parameters, like the packing fraction, attractive strength, particle size, on the cluster formation in the system. The general shapes of the pair connectedness are similar to the one component sticky situation. Also the unphysical result of the percolation line approaching a finite value as density tends to zero still held as in the one component SHS result. This meant that the system will percolate even at vanishingly small density [9].

The present work also attempts to investigate percolation in binary mixtures of SHS, but the situation considered here is that the interaction between unlike particles is SHS, while hard sphere repulsion is found amongst the same species. The definition for connectivity is the overlap of particle cores. Since the bound energy between like particles is zero, the clustering is also selective. The 'physics' is quite different from the system studied by Chiew and Glandt [14]. We find that the percolation line goes to zero as density approaches zero and there can be lower limits on the density at some special conditions; below these limits percolation is impossible. Usually the curves of mean cluster size rise drastically as the density approaches percolation threshold, which indicates the clustering procedure in this system is not gradually developed. By solving the OZ equation, which is a group of coupled integral equations here, the pair connectedness functions exhibit different behaviours compared with Chiew and Glandt's [14] results. Another gauge of the extent of aggregation is the partial coordination number $Z_{ij}(r_1)$ [15] which is defined as the average number of type- j particles within a distance r_1 of a type- i particle. The effects of changing stickiness and ratio of diameters on Z_{ij} are examined.

The article is organized as follows. The model as well as relevant formulas are presented in section 2. Section 3 gives the expressions of physical quantities used to discuss percolation. The results and analyses are reported in section 4. Conclusions and possible extensions are given in the last section.

2. The model

We consider a system of two components with number density ρ_i , $i = 1, 2$. Baxter's [16] SHS potential, according to Barbov's [17] convention, can be defined as

$$\exp(-\beta u_{ij}(r)) = \begin{cases} (d_{ij}/2\tau_{ij})\delta(r - d_{ij}) & 0 < r \leq d_{ij} \\ 1 & r > d_{ij} \end{cases} \quad (1)$$

where β is the inverse of Boltzmann's constant times the temperature T , τ_{ij} are stickiness parameters which can be considered as dimensionless measure of temperature with $\tau_{ij}^{-1} \rightarrow 0$ corresponding to hard sphere interaction. Diameters of particles are assumed additive and satisfy

$$d_{ij} = (d_{ii} + d_{jj})/2. \quad (2)$$

The transformation of the OZ equation for mixtures is given by Baxter [18] and can be solved analytically by the factorization method [19]. By virial expansions of the pair distribution functions $g_{ij}(r)$, we can write [17]

$$g_{ij}(r) = \frac{t_{ij}}{d_{ij}} \delta(r - d_{ij}) \quad 0 < r \leq d_{ij} \quad (3)$$

where

$$t_{ij} = \frac{\lambda_{ij} d_{ii} d_{jj}}{12(1 - \xi_3)} \quad (4)$$

$$\xi_\alpha = \frac{\pi}{6} \sum_{i=1}^2 \rho_i d_{ii}^\alpha. \quad (5)$$

The equations to determine the parameters λ_{ij} are

$$\tau_{ij} \lambda_{ij} = \frac{9d_{ij}\xi_2}{1 - \xi_3} + \frac{6d_{ij}^2}{d_{ii}d_{jj}} + \frac{\pi d_{ij}}{12(1 - \xi_3)} \sum_{k=1}^2 \rho_k d_{kk} (\lambda_{ik} \lambda_{jk} - 6\lambda_{ik} - 6\lambda_{jk}). \quad (6)$$

This equation is crucial in the study the phase behaviour of the system.

Only unlike particles interact by sticky attraction and the hard sphere potential acts among particles of the same species; that is τ_{12} is to be a finite value, while $\tau_{11}, \tau_{22} \rightarrow \infty$, equation (6) then becomes

$$\lambda_{11} = \lambda_{22} = 0 \quad (7)$$

$$\lambda_{12} = 3 \left(\frac{3d_{12}\xi_2/(1 - \xi_3) + 2d_{12}^2/d_{11}d_{22}}{3d_{12}\xi_2/(1 - \xi_3) + \tau_{12}} \right). \quad (8)$$

According to Barbov [20], the system cannot exhibit discontinuous phase separation since λ_{12} is finite and continuous within the physically allowable density range $0 < \xi_3 < 1$. However, by the requirement of convergence of the total correlation function, λ_{12} has to satisfy

$$\lambda_{12} < 3 + \left[\left(3 + \frac{1 - \xi_3}{\eta_1} \right) \left(3 + \frac{1 - \xi_3}{\eta_2} \right) \right]^{1/2} \quad (9)$$

where $\eta_i = \pi\rho_i d_{ii}^3/6$ is the packing fraction of the i th species. Therefore, the conclusion drawn by Barbooy is that there exists a ‘critical temperature’ τ_{12}^c depending on concentration and ratio of particle diameters, where a fluid-fluid discontinuous transition between states of different concentrations and densities will occur when $\tau_{12} < \tau_{12}^c$ if the difference of particle size is large.

We give the expression for τ_{12}^c explicitly by equation (8) and equation (9)

$$\tau_{12}^c = \frac{3[3d_{12}\xi_2/(1-\xi_3) + 2d_{12}^2/d_{11}d_{22}]}{3 + \sqrt{[3 + (1-\xi_3)/\eta_1][3 + (1-\xi_3)/\eta_2]}} - \frac{3d_{12}\xi_2}{1-\xi_3} \tag{10}$$

The relation with percolation ‘temperature’ will be examined in the final section.

3. Connectivity and percolation of the model

We list below the extension to mixtures of Coniglio’s formulation derived by Chiew and Stell [12] for convenience.

The pair connectedness for isotropic systems, $p_{ij}(r)$, is defined such that $\rho_i\rho_j p_{ij}(|r_1 - r_2|) dr_1 dr_2$ is the probability that two particles from components i and j are in volume elements dr_1, dr_2 simultaneously and physically bound. $p_{ij}(r)$ satisfies the OZ equation

$$rp_{ij}(r) = -q'_{ij}(r) + 2\pi \sum_k \rho_k \int_{s_{ik}}^{d_{ik}} q_{ik}(t)(r-t)p_{jk}(|r-t|) dt \quad r > s_{ij} \tag{11}$$

Here s_{ij} is defined as

$$s_{ij} = (d_{ii} - d_{jj})/2. \tag{12}$$

Boltzmann’s factor can be divided into two parts

$$\exp(-\beta u_{ij}(r)) = \exp(-\beta u_{ij}^\dagger(r)) + \exp(-\beta u_{ij}^*(r)) \tag{13}$$

where $u_{ij}^\dagger(r)$ and $u_{ij}^*(r)$ are potentials for pairs of bound and unbound particles respectively.

The PY approximation can be expressed as

$$p_{ij}(r) = \exp(-\beta u_{ij}^\dagger(r))g_{ij}(r) \exp(\beta u_{ij}(r)) + \exp(-\beta u_{ij}^*(r))(p_{ij}(r) - c_{ij}^\dagger(r)) \tag{14}$$

where direct connectedness $c_{ij}^\dagger(r)$ is the non-nodal graphs of p_{ij} ’s graphic expansion.

Define

$$\bar{q}_{ij}(k) = \delta_{ij} - 2\pi \sqrt{\rho_i\rho_j} \int_{s_{ij}}^{d_{ij}} \exp(ikr)q_{ij}(r) dr. \tag{15}$$

The mean cluster size S is given by

$$S = 1 + \sum_i \sum_j c_i \sqrt{\rho_j/\rho_i} \{[\bar{q}(0)^{-1}\bar{q}^T(0)^{-1}]_{ij} - \delta_{ij}\} \tag{16}$$

where $c_i = \rho_i/\rho$, $\rho = \rho_1 + \rho_2$, $\bar{q}^T(0)^{-1}$ is the transpose of the inverse matrix of $(\bar{q}_{ij}(0))$. The percolation threshold is the density at which S is divergent.

Our solution of the percolation problem for the present system is listed as follows.

With the core overlap defined as two particles being bound physically, it can be shown that

$$\exp(-\beta u_{ij}^\dagger(r)) = (d_{ij}/2\tau_{ij})\delta(r - d_{ij})(1 - \delta_{ij}) \quad (17)$$

$$\exp(-\beta u_{ij}^*(r)) = \theta(r - d_{ij}). \quad (18)$$

Here $\theta(r - d_{ij})$ is the Heaviside step function. By the PY approximation

$$p_{ij}(r) = (t_{ij}/d_{ij})\delta(r - d_{ij})(1 - \delta_{ij}) \quad r \leq d_{ij} \quad (19)$$

and equation (11) is changed into

$$q'_{ij}(r) = -t_{ij}\delta(r - d_{ij})(1 - \delta_{ij}) \quad s_{ij} < r < d_{ij}. \quad (20)$$

Using the condition

$$q_{ij}(r \geq d_{ij}) = 0 \quad (21)$$

we obtain, after trivial integration

$$q_{ij}(r) = \begin{cases} t_{ij}(1 - \delta_{ij}) & s_{ij} < r < d_{ij} \\ 0 & r < s_{ij} \text{ or } r \geq d_{ij}. \end{cases} \quad (22)$$

Substituting (22) into (15) and letting $q = 0$, we find

$$\bar{q}_{ij}(0) = \delta_{ij} - 2\pi\sqrt{\rho_i\rho_j}t_{ij}d_{ij}(1 - \delta_{ij}). \quad (23)$$

We transform equation (16) into

$$S = \frac{1}{|\det \bar{q}(0)|^2} \left\{ c_1 \left[\bar{q}_{22}(0) - \left(\frac{\rho_2}{\rho_1} \right)^{1/2} \bar{q}_{21}(0) \right]^2 + c_2 \left[\bar{q}_{11}(0) - \left(\frac{\rho_1}{\rho_2} \right)^{1/2} \bar{q}_{12}(0) \right]^2 \right\}. \quad (24)$$

Inserting equations (4) and (23) into (24), the result is

$$S = \frac{1}{|\det \bar{q}(0)|^2} \left\{ c_1 \left[1 + \frac{\eta_2}{(1 - \xi_3)} \left(\frac{d_{11}}{d_{22}} \right)^2 \lambda_{12} \right]^2 + c_2 \left[1 + \frac{\eta_1}{(1 - \xi_3)} \left(\frac{d_{22}}{d_{11}} \right)^2 \lambda_{12} \right]^2 \right\} \quad (25)$$

where

$$\det \bar{q}(0) = 1 - \frac{\eta_1 \eta_2 \lambda_{12}^2}{(1 - \xi_3)^2}. \quad (26)$$

The percolation threshold is determined by

$$\det \bar{q}(0) = 0. \quad (27)$$

By combining equations (26), (27) and (8), we obtain the expression for the percolation line

$$\tau_{12}^p = \frac{\sqrt{\eta_1 \eta_2}}{1 - \xi_3} \left(\frac{9d_{12}\xi_2}{1 - \xi_3} + \frac{6d_{12}^2}{d_{11}d_{22}} \right) - \frac{3d_{12}\xi_2}{1 - \xi_3}. \quad (28)$$

The partial coordination number Z_{12} , which is the average number of type-2 particles that contact with a type-1 particle directly due to the δ -function singularity in g_{ij} , can be obtained easily by integrating equation (3)

$$Z_{12} = \frac{2d_{11}d_{12}}{d_{22}^2(1 - \xi_3)} \lambda_{12}\eta_2 \quad (29)$$

Substituting equation (20) into equation (11), the OZ equations for $p_{ij}(r)$ are a group of coupled integral equations

$$r p_{11}(r) = 2\pi \rho_2 \int_{s_{12}}^{d_{12}} q_{12}(t)(r-t)p_{12}(|r-t|) dt \quad \text{for } r > 0 \quad (30)$$

$$r p_{22}(r) = 2\pi \rho_1 \int_{s_{21}}^{d_{21}} q_{21}(t)(r-t)p_{21}(|r-t|) dt \quad \text{for } r > 0 \quad (31)$$

$$r p_{12}(r) = \frac{d_{11}d_{22}\lambda_{12}}{12(1 - \xi_3)} \delta(r - d_{12}) + 2\pi \rho_2 \int_{s_{12}}^{d_{12}} q_{12}(t)(r-t)p_{22}(|r-t|) dt \quad \text{for } r > s_{12}. \quad (32)$$

We have solved the OZ equations, in conjunction with (19), using the algorithm due to Perram [21]. All results and discussion are presented in the next section.

4. Results and discussion

The non-singular part of pair connectedness functions are presented in figures 1–6. These have been obtained by the solution of the OZ equation by Perram's algorithm. As can be seen from figures 1–3, general shapes of $p_{11}(r)$ and $p_{22}(r)$ are similar to the one component SHS cases [9, 10, 14]. This is due to two like particles being connected by intermediate unlike particles with interaction potential SHS. The function $p_{12}(r)$ has a quite different shape since in this situation, a chosen component-2 particle plays the role of 'adsorption' centre of the hard sphere particles. These shapes for $p_{12}(r)$ are shown in figures 4–6 as well the previous figures.

Figure 1, together with figures 2 and 3, shows the discontinuities in $p_{11}(r)$ and $p_{22}(r)$ due to the influence of the delta function in $p_{12}(|r-t|)$ occurring at $r = d_{11}$, d_{22} and $d_{11} + d_{22}$. This delta function also determines the discontinuities of the derivative in $p_{12}(r)$ as shown in figures 4–6. It can easily be shown that these occur at $r = d_{11} + d_{22}$, $d_{22} + d_{12}$ and $d_{11} + d_{22} + d_{12}$. This is confirmed by the computations.

The pair connectedness at percolation density is shown in figure 2, all other conditions being the same as in figure 1. All these three functions become long range as expected.

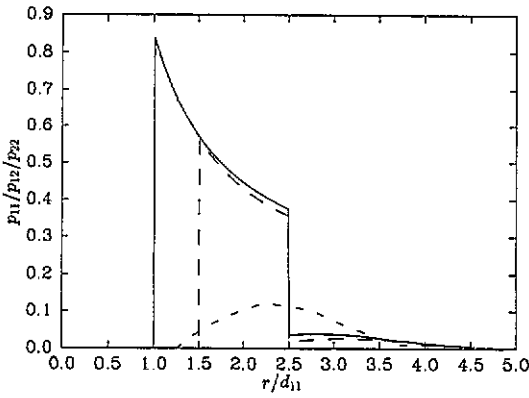


Figure 1. Pair-connectedness (non-singular part) p_{11} , p_{12} and p_{22} with parameters $d_{22}/d_{11} = 1.5$, $c_1 = 0.5$, $\tau_{12} = 0.2$, $\rho = 0.039$. Full curve, p_{11} ; broken curve, p_{12} ; long broken curve, p_{22} .

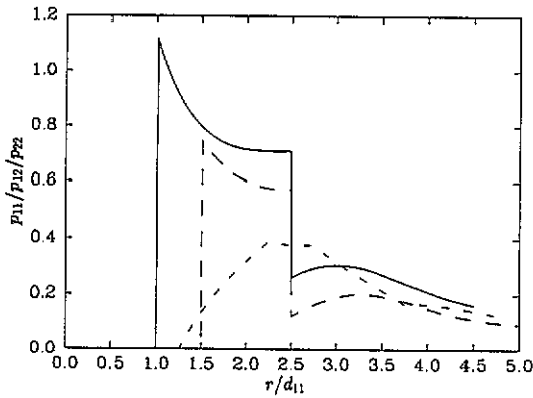


Figure 2. As figure 1, but for $\rho = 0.147$ (close to the percolation threshold).

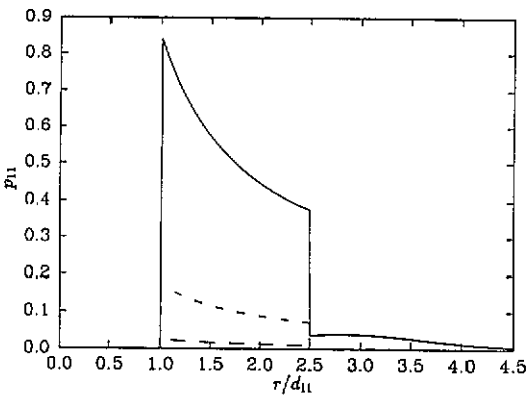


Figure 3. Pair-connectedness p_{11} (non-singular part) for different stickiness with other parameters as in figure 1. Full curve, $\tau_{12} = 0.12$; broken curve, $\tau_{12} = 0.6$; long broken curve, $\tau_{12} = 1.8$.

The influence of stickiness on $p_{11}(r)$ is shown in figure 3. $p_{11}(r)$ decreases rapidly as the decrease of stickiness. Similar behaviour can be found for $p_{22}(r)$ and $p_{12}(r)$. Also note the same effect in figure 4 on $p_{12}(r)$; as τ_{12} increases the pair connectedness

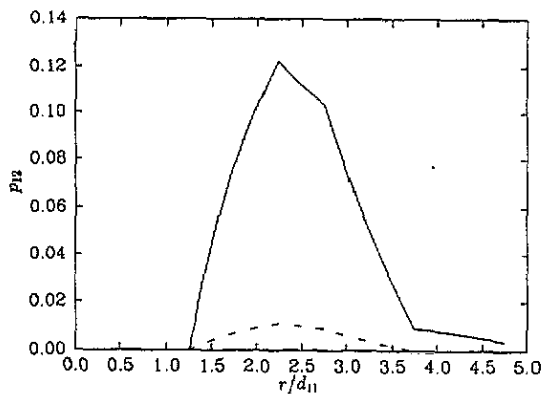


Figure 4. Pair-connectedness p_{12} (non-singular part) with parameters as in figure 1.

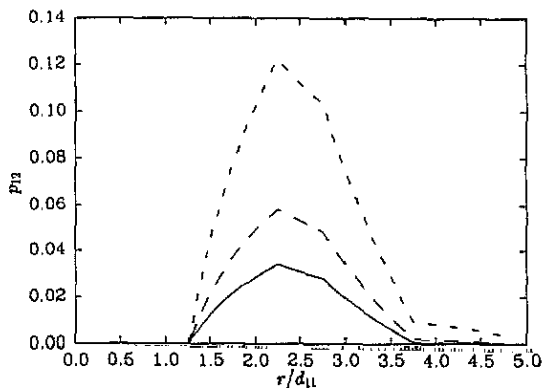


Figure 5. Pair-connectedness p_{12} (non-singular part) for different concentration with other parameters as in figure 1. Full curve, $c_1 = 0.1$; broken curve, $c_1 = 0.5$; long broken curve, $c_1 = 0.9$.

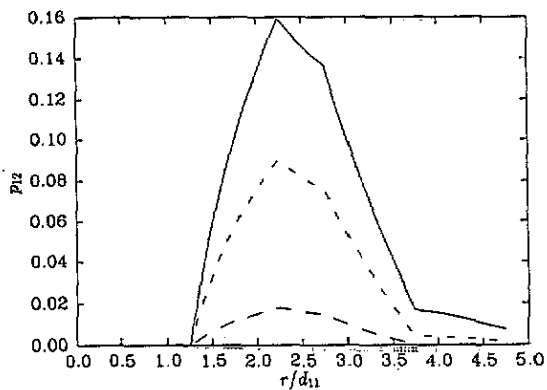


Figure 6. Pair-connectedness p_{12} (non-singular part) for different densities with other parameters as in figure 1. Full curve, $\rho = 0.05$; broken curve, $\rho = 0.03$; long broken curve, $\rho = 0.01$.

function tends to the hard sphere value, i.e. vanishing everywhere. Figures 5 and 6 respectively show the effect of change in concentration and the change of the total density of the system. The effect of concentration shows the change in connectivity

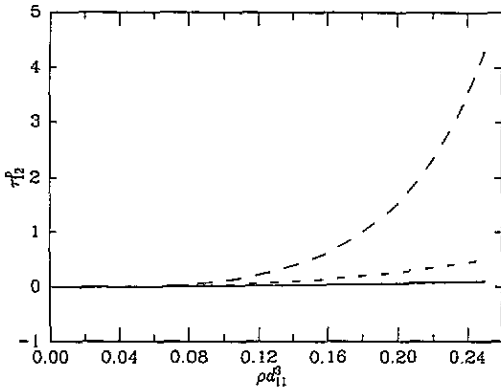


Figure 7. Percolation line τ_{12}^P for $c_1 = 0.5$. Full curve, $d_{22}/d_{11} = 1.0$; broken curve, $d_{22}/d_{11} = 1.5$; long broken curve, $d_{22}/d_{11} = 2$.

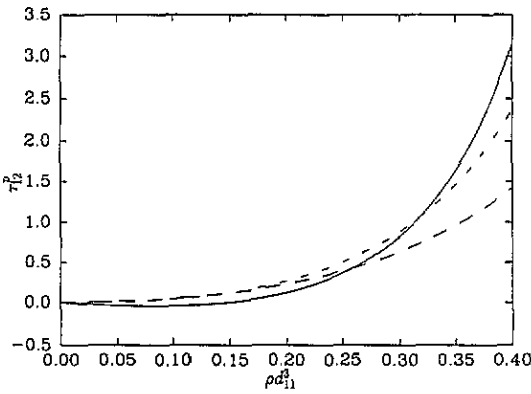


Figure 8. τ_{12}^P for $d_{22}/d_{11} = 1.5$. Full curve, $c_1 = 0.3$; broken curve, $c_1 = 1.0$; long broken curve, $c_1 = 0.7$.

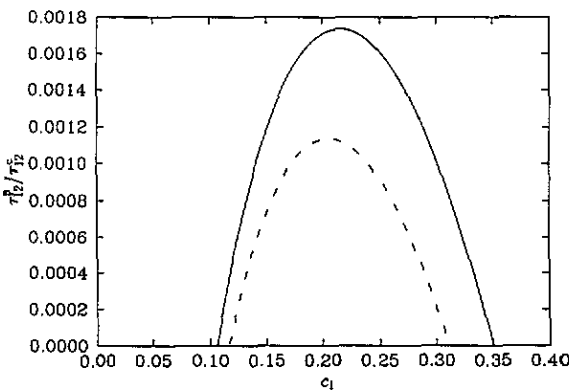


Figure 9. Percolation line τ_{12}^P and phase transition line τ_{12}^c for $d_{22}/d_{11} = 0.5$, $\rho = 0.05$. Full curve, τ_{12}^c ; broken curve, τ_{12}^P .

with change in concentration. The decrease in connectivity is due to the reduced effect of the attraction between unlike particles—the magnitude of this decrease being affected by the ratio of diameters. In the case of the lowering of density the

connectivity again decreases.

Different features of the percolation line, defined by equation (28) are displayed in figures 7 to 9.

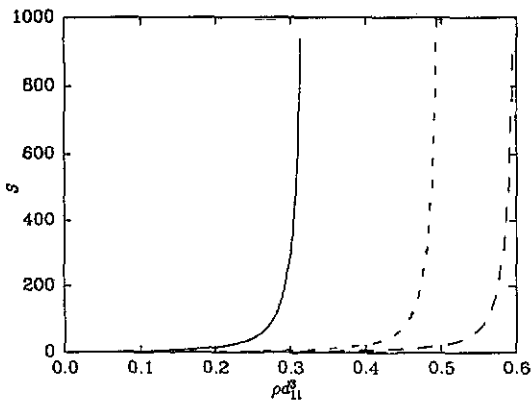


Figure 10. Mean cluster size S with parameters $d_{22}/d_{11} = 1.0$, $c_1 = 0.5$. Full curve, $\tau_{12} = 0.2$; broken curve, $\tau_{12} = 0.6$; long broken curve, $\tau_{12} = 1.0$.

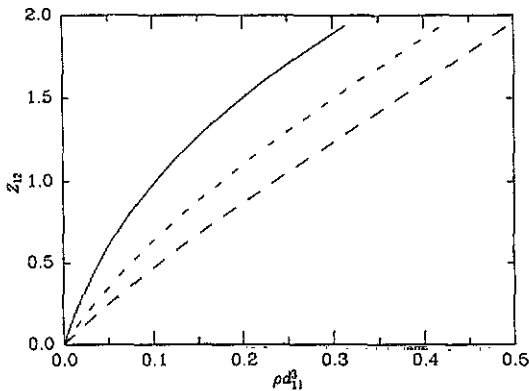


Figure 11. Coordination number Z_{12} for $d_{22}/d_{11} = 1.0$, $c_1 = 0.5$. Full curve, $\tau_{12} = 0.2$; broken curve, $\tau_{12} = 0.4$; long broken curve, $\tau_{12} = 0.6$.

When considering the one component SHS system [4] and also the binary mixtures with strong attraction between like species [14], the percolation line was found to approach a finite value when the density went to zero which meant that percolation always occurred for these systems even at zero density—an unphysical result. The result for the present system is quite different. The percolation line always goes to zero as density vanishes. Figure 7 shows that the percolation threshold increases as the ratio of diameters decreases. Figure 8 shows the percolation lines for differing concentrations keeping the ratio of diameters fixed. For the case displayed by the broken curve in figure 7 and full curve in figure 8, it is apparent that there exist lower limits of density below which percolation never occur, i.e. where the percolation line becomes negative.

A plot of percolation ‘temperature’ τ_{12}^p against c_2 at fixed density is shown in figure 9. The percolation area is the portion enclosed by the percolation line with concentration as the variable. Figure 9 shows that there is a range of concentration

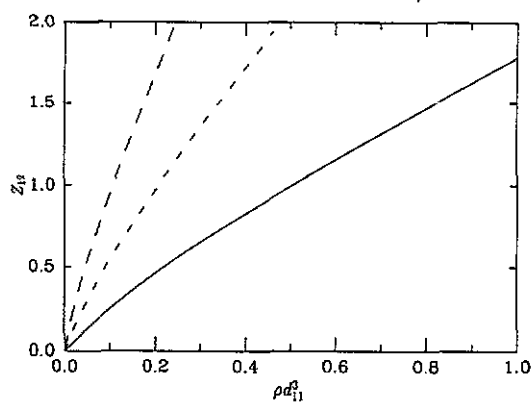


Figure 12. Z_{12} with $c_1 = 0.5$, $\tau_{12} = 0.5$. Full curve, $d_{22}/d_{11} = 0.5$; broken curve, $d_{22}/d_{11} = 1.0$; long broken curve, $d_{22}/d_{11} = 1.5$.

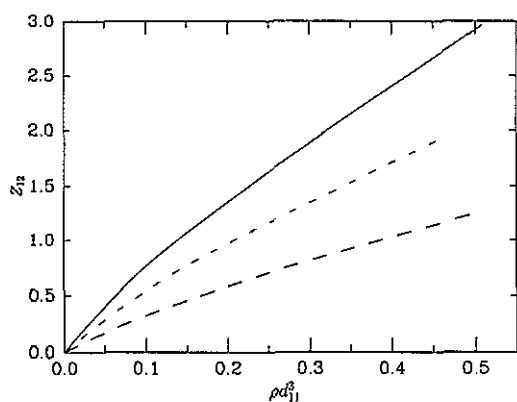


Figure 13. Z_{12} for different concentration with $d_{22}/d_{11} = 1.0$, $\tau_{12} = 0.5$. Full curve, $c_1 = 0.3$; broken curve, $c_1 = 0.5$; long broken curve, $c_1 = 0.7$.

beyond which percolation is impossible. The phase transition line, expressed by equation (10) [20], is given by the broken curve which lies totally within the percolation area. The area enclosed by the phase transition line is unphysical due to the divergence of the total correlation functions and will diminish as the ratio of diameters increases [20]—this further restricts the values of concentration for which percolation can occur.

Bug *et al* [22] have observed by Monte Carlo studies for square-well systems that increase of attraction can either raise or lower the percolation threshold. The main reason, indicated by Seaton and Glandt [9, 10] is their more liberal definition of connectivity. Because the definition of core-overlap connectivity is used here, figure 10 shows that increasing attraction, i.e. increasing stickiness, always lowers the percolation threshold.

The partial coordination number Z_{12} is plotted as a function of reduced density ρd_{11}^3 for different values of stickiness in figure 11, for different ratios of diameters in figure 12 and for different concentrations in figure 13. Figure 11 displays that Z_{12} increases with increasing τ_{12} for fixed density as it should be. Figure 12 shows the effect of the ratio of diameters on Z_{12} at constant stickiness and concentration. The influence of concentration on Z_{12} is displayed in figure 13, Z_{12} decreases as c_1

increases (i.e. c_2 decreases) for a given density and stickiness. All curves show that Z_{12} is a monotonically increasing function of the density.

5. Conclusion

Several new features appeared in the present system when percolation is studied. Concentration plays a more important role than in Chiew and Glandt's [14] model. With the 'extended sphere' [13] as the definition of connectivity of two like particles, it is possible to observe that the increase of attraction may raise or lower percolation threshold, the difficult point of this extension is to solve the coupled OZ equations analytically in order to find closed expressions for $g_{ii}(r)$ $i = 1, 2$ in the second shell $d_{ii} < r < 2d_{ii}$. Another possible extension of the present model is to take the 'permeable sphere' as the potential of like particles; structure, thermodynamics and percolation could then be studied. Generally speaking, percolation or 'compound forming' should be easier in this case since repulsion between like particles is not as strong as the hard sphere potential. One more input parameter is needed for both possible extensions mentioned above.

Acknowledgments

One of us (MS) gratefully acknowledges discussions with S Baer and B Barboj.

References

- [1] Barboj B 1978 *Chem. Phys.* **34** 231
- [2] Hill T L 1955 *J. Chem. Phys.* **23** 617
- [3] Coniglio A, De Angelis U, Forlani A and Lauro G 1977 *J. Phys. A: Math. Gen.* **10** 219
- [4] Coniglio A, De Angelis U and Forlani A 1977 *J. Phys. A: Math. Gen.* **10** 1123
- [5] Chiew Y C and Glandt E D 1983 *J. Phys. A: Math. Gen.* **16** 2599
- [6] De Simone T, Demonlini S and Stratt R M 1986 *J. Chem. Phys.* **85** 391
- [7] Xu J and Stell G 1988 *J. Chem. Phys.* **89** 1101
- [8] Netemeyer S C and Glandt E D 1986 *J. Chem. Phys.* **85** 6054
- [9] Seaton N A and Glandt E D 1987 *J. Chem. Phys.* **86** 4668
- [10] Seaton N A and Glandt E D 1987 *Phys. Chem. Hydro.* **9** 369
- [11] Chiew Y C and Wang Y H 1988 *J. Chem. Phys.* **89** 6385
- [12] Chiew Y C, Stell G and Glandt E D 1985 *J. Chem. Phys.* **83** 761
- [13] Wu G and Chiew Y C 1989 *J. Chem. Phys.* **90** 5024
- [14] Chiew Y C and Glandt E D 1989 *J. Phys. A: Math. Gen.* **22** 3969
- [15] Cusack N E 1987 *The Physics of Structurally Disordered Matter: An Introduction* (Bristol: Adam Hilger) p 36
- [16] Baxter R J 1968 *J. Chem. Phys.* **49** 2770
- [17] Barboj B 1975 *Chem. Phys.* **11** 357
- [18] Baxter R J 1970 *J. Chem. Phys.* **52** 4559
- [19] Baxter R J 1968 *Aust. J. Phys.* **21** 563
- [20] Barboj B and Tenne R 1979 *Chem. Phys.* **38** 369
- [21] Perram J W 1975 *Mol. Phys.* **30** 1505
- [22] Bug A L R, Safran S A and Grest G S 1985 *Phys. Rev. Lett.* **55** 1896